A compact equivalent circuit for the dark current-voltage characteristics of nonideal solar cells

J. Pallarès, R. Cabré, L. F. Marsal, and R. E. I. Schropp

Citation: Journal of Applied Physics **100**, 084513 (2006); doi: 10.1063/1.2357641
View online: http://dx.doi.org/10.1063/1.2357641
View Table of Contents: http://scitation.aip.org/content/aip/journal/jap/100/8?ver=pdfcov
Published by the AIP Publishing

A compact equivalent circuit for the dark current-voltage characteristics of nonideal solar cells

J. Pallarès,[a] R. Cabré, and L. F. Marsal
Departament d'Enginyeria Electrònica, Universitat Rovira i Virgili, Avinguda Països Catalans, 26, 43007 Tarragona, Spain

R. E. I. Schropp
Debye Institute, Utrecht University, P.O. Box 80000, NL-3508 TA, Utrecht, The Netherlands

(Received 22 March 2006; accepted 5 July 2006; published online 31 October 2006)

This paper presents a compact electrical equivalent circuit which describes the dark current-voltage characteristics of nonideal *p-n* junction solar cells in a wide range of temperatures. The model clearly separates the voltage drop in the junction and bulk regions. It is based on the combination of two exponential mechanisms, shunt and series resistances and space-charge limited current. In order to increase the accuracy of the parameter extraction process, both ln(*I-V*) and its derivative plots are fitted simultaneously. From the temperature dependence of the extracted parameters, the conduction mechanisms governing the *I-V* characteristics can be obtained without assuming dominating terms. In addition, the extracted parameters can be related to other electrical magnitudes obtained from such independent measurements as capacitance-voltage measurements (diffusion potential) and illuminated current-voltage characteristics (series resistance and open-circuit voltage). To exemplify the application, a p^+ *a*-SiC:H/*n c*-Si solar cell is studied and a number of major physical aspects derived from the analysis of the fitting values are discussed. © *2006 American Institute of Physics*. [DOI: 10.1063/1.2357641]

I. INTRODUCTION

Several equivalent circuits have been proposed to describe the current-voltage (*I-V*) characteristics of solar cells, all of which are based on the superposition of the photocurrent source (I_{PH}) on the characteristics of the dark diode. For an ideal crystalline *p-n* solar cell, the dark diode consists of a diode shunting I_{PH}, which describes the drift-diffusion losses, and the series and shunt resistances, R_S and R_{SH}, respectively.[1] When dealing with nonideal *p-n* junction solar cells, this ideal model is usually modified by including additional parasitic series and parallel conductances[2] or a second exponential term which takes into account other conduction mechanisms such as recombination[3] or tunneling processes.[4] In a particular device, the actual conduction mechanism related to each exponential term can be obtained by analyzing its temperature dependence.

But this classical analysis does not take into account other conduction mechanisms, most of which are described by a nonlinear current-voltage dependence and have been recently reported in GaAs concentrator solar cells,[5] copper indium gallium diselenide (CIGS) solar cells,[6] and organic solar cells.[7] Of all the possible conduction mechanisms with a nonlinear current-voltage dependence, the space-charge limited current (SCLC) mechanism[8] has recently been reported not only in organic solar cells[9–14] but also in amorphous germanium solar cells[15] and porous nanocrystalline TiO_2 layers.[16] In addition, the SCLC mechanism has also been reported in *a*-SiC:H/*c*-Si diodes,[17] *a*-SiGe/*c*-Si diodes,[18] *a*-Si nanoparticles,[19] Si nanocrystals,[20] CdSe/ZnS quantum dots,[21] organic semiconductors,[22] and high-*k* insulators.[23]

The SCLC can be described by the relationship $I=kV^m$, where *m* is related to the density of states (DOS) of the transport path ($m=2$ for a SCLC without traps and $m>2$ with traps), and *k* is related to the film thickness, trap distribution, and conductivity of the transport path.

If this SCLC dependence were to be included in the current-voltage relationship together with the exponential terms and the series and shunt resistance, the voltage junction drop would not be explicit. As a first step to solving this problem, Marsal *et al.*[24] proposed for *a*-Si:H/*c*-Si diodes that the junction effects should be separated from the amorphous bulk region effects and they designed a parameter extraction method based on an equivalent circuit consisting of an ideal diode in series with a parallel combination of an Ohmic and a nonlinear resistance (SCLC term).

In this paper we present a compact electrical equivalent circuit which describes the dark current density-voltage-temperature characteristics of nonideal junction solar cell. The circuit includes two exponential mechanisms, shunt and series resistances and a SCLC term. As an example of an application, we study a $p+$*a*-SiC:H/*n c*-Si solar cell and extract the fitting parameters. And finally, we discuss the major physical aspects of the parameters extracted from the analysis and compare the results with those obtained for the same sample by capacitance-voltage measurements and illuminated current-voltage characteristics.

[a]Electronic mail: josep.pallares@urv.cat

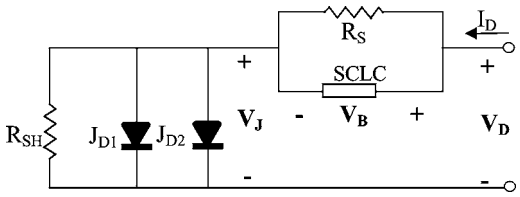

FIG. 1. Electrical equivalent circuit.

II. EQUIVALENT CIRCUIT

Figure 1 shows the compact equivalent circuit proposed in this article. For a given applied voltage, V_D, the goal of the extraction parameter procedure is to calculate the drop voltage in the junction, V_J, and the drop voltage in the bulk, V_B. Then,

$$V_D = V_J + V_B. \tag{1}$$

The bulk voltage drop is due to the parallel combination of the series resistance R_S and the SCLC term. So the total current I_D is divided into two terms

$$I_D = I_{R_S} + I_{\mathrm{SCLC}} = \frac{V_B}{R_S} + kV_B{}^m, \tag{2}$$

where k and m are the SCLC parameters.

The junction voltage drop is due to the parallel combination of the two exponential terms, namely, I_{D1} and I_{D2}, and the shunt resistance R_{SH}. So the total current can also be expressed as

$$I_D = I_{D1} + I_{D2} + I_{\mathrm{RSH}} = \sum_{i=1}^{2} I_{\mathrm{Si}}[\exp(A_i V_J) - 1] + \frac{V_J}{R_{\mathrm{SH}}}, \tag{3}$$

where $I_{S1,2}$ and $A_{1,2}$ are the reverse saturation current and the exponential factor of the two exponential currents, respectively. Equation (3) coincides with the two-diode model if SCLC effects are neglected ($k=0$), i.e., $V_J=V_D-I_DR_S$.

The set of Eqs. (1)–(3) is self-consistent and enables the eight fitting parameters (I_{S1}, I_{S2}, A_1, A_2, R_S, R_{SH}, k, and m) to be calculated simultaneously. Although there might be many fitting parameters, they are all needed to describe the dark current-voltage-temperature characteristics if all the above mentioned conduction mechanisms are taken into account. To improve the accuracy of the parameter extraction process, we propose to fit both $\ln I$ vs V and $d(\ln I)/dV$ vs V plots simultaneously because this enables unrealistic fitting parameters to be eliminated. In addition, it should be pointed out that the total current is not limited simultaneously by all the possible conduction mechanisms throughout the voltage range studied but by one or two conduction mechanisms, as we shall discuss in the application section.

From the dependence temperature of the fitting parameters, it is possible to elucidate the actual conduction mechanisms governing the forward dark current-voltage characteristics. There is no need to assume that there is one dominant current term because the same model applies throughout the range of applied voltages. Although the model is developed to describe the dark forward characteristics of solar cells, it is also useful for reverse voltages if the device is limited by shunt resistance.

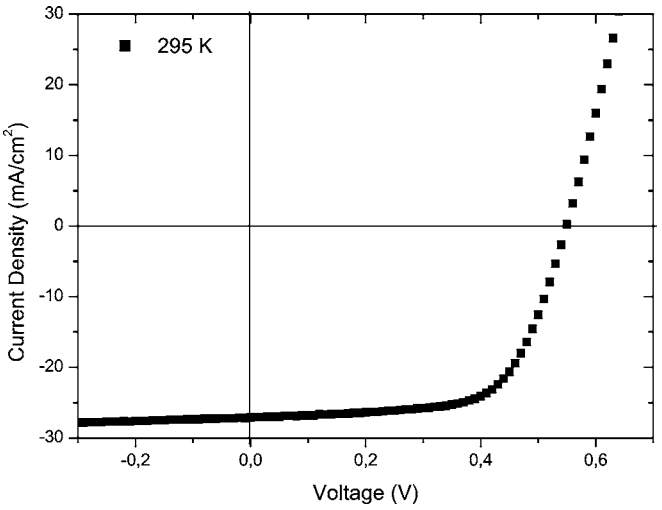

FIG. 2. Experimental current-voltage characteristics of the $p+a$-SiC:H/n c-Si solar cell under AM1.5 illumination.

III. APPLICATION AND DICUSSION

In order to check the validity of the equivalent circuit proposed here, we studied the dark current-voltage-temperature (I-V-T) characteristics of a $p+a$-SiC:H/n c-Si solar cell. Details about the fabrication of the sample can be found elsewhere.[25] Figure 2 shows the experimental current-voltage characteristics of the solar cell under AM 1.5 illumination. The measured values of the solar cell parameters are V_{OC}=548 mV, J_{SC}=27.1 mA/cm^2, FF=0.654, η=9.7%, R_{S} =4.9 Ω, and R_{SH}=612 Ω.

Figure 3 shows the experimental and fitted dark I-V-T characteristics (a) and the experimental and fitted curves for $d(\ln I)/dV$ vs V (b) for the same solar cell. The equivalent circuit describes the experimental data throughout the temperature range studied. Although the derivative plot is extremely sensitive to the fitting parameters, particularly to the reverse saturation current and the exponential factor of the two exponential currents, the agreement is good.

Figure 4 shows the experimental and the best fitting results for the ln(I-V) (a) and its derivative (b) of the same diode at room temperature but taking into account only one exponential mechanism, shunt and series resistances (simplified model). The fitting curve does not follow the experimental data in either the low or high forward regions, specially for the derivative plot. This result shows the importance of including the second exponential mechanism and the SCLC term in the electrical model.

Figure 5 shows the contribution of the different conduction mechanisms to the total current at room temperature. The plot clearly demonstrates that for each voltage range the total current is dominated by particular conduction mechanisms, the shunt resistance and one exponential term limit the reverse voltage and the low forward voltage regions ($V_D<0.4$ V), the other exponential term and the series resistance limit the medium forward voltage region [$0.4<V_D(\mathrm{V})<0.7$], and the excess current in the high forward bias range ($V_D>0.7$ V) can be explained by SCLC effects. That means that the fitting parameters R_{SH}, I_{S2}, and A_2 are extracted from the reverse and low forward voltage regions,

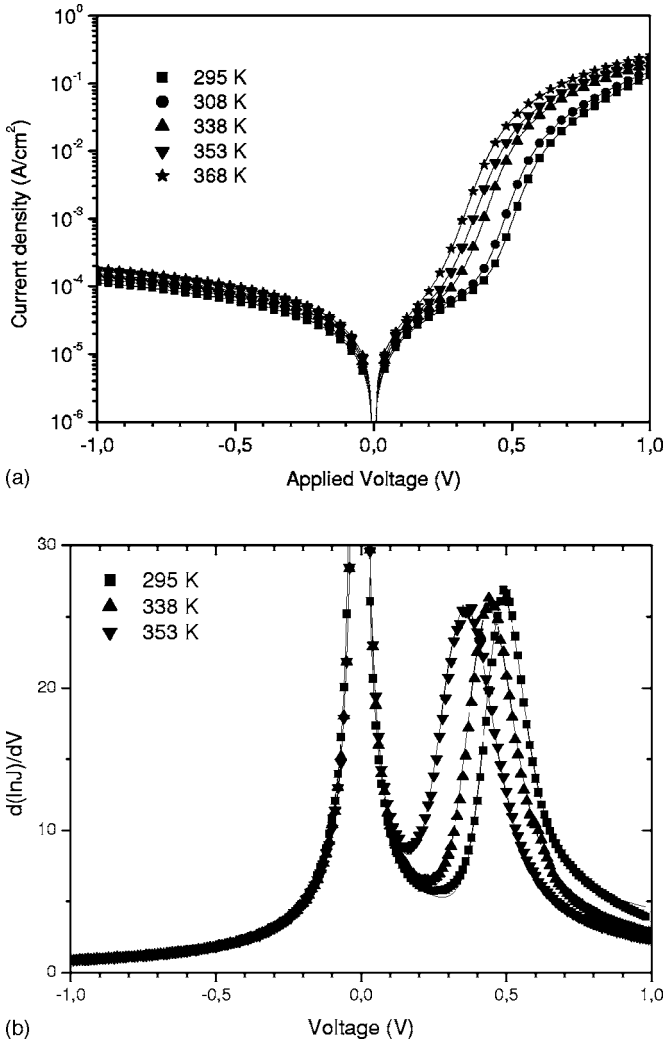

FIG. 3. Experimental (symbols) and fitted (line) dark current-voltage-temperature plot (a) and its derivative (b) of the solar cell from Fig. 2. The compact model proposed in this work has been used.

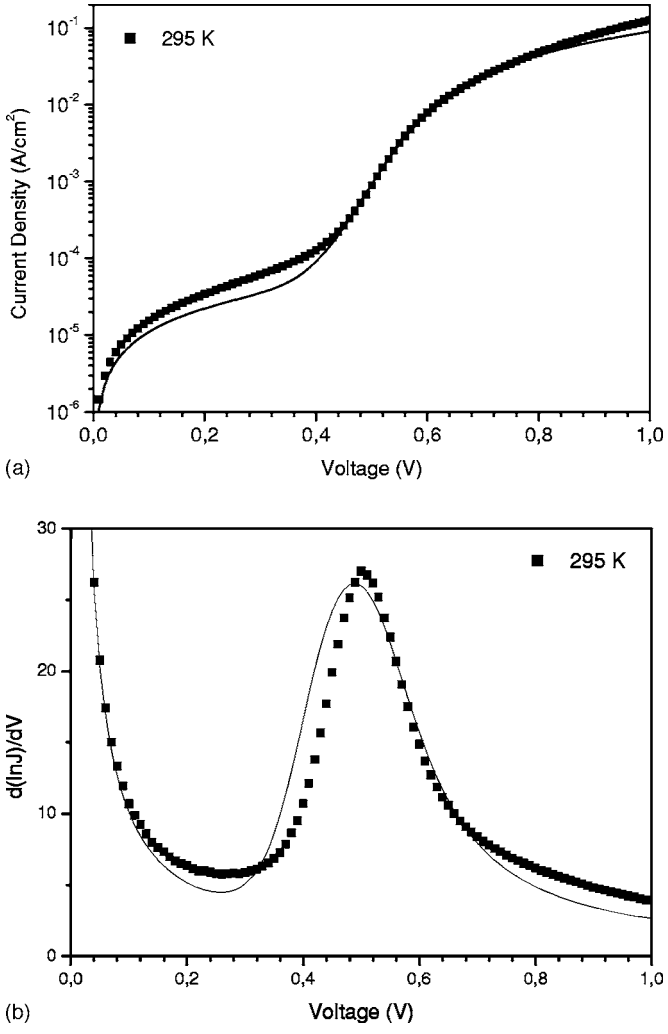

FIG. 4. Experimental (symbols) and fitted (line) dark current-voltage plot (a) and its derivative (b) of the solar cell from Fig. 2 at room temperature. The simplified model has been used.

while the fitting parameters R_S, I_{S1} and A_1 are extracted from the medium forward voltage region and the fitting parameters k and m are extracted from the high voltage region.

In the reverse and low forward voltages ($V_D < 0.4$ V), the current due to the exponential term with a high saturation reverse current density ($J_{S2}=6.8\ \mu A/cm^2$) and low exponential factor ($A_2=5.4$) is in the same order of magnitude as the shunt current term ($R_{SH}=9\ k\Omega$) at room temperature. Nevertheless, both terms are needed to fit the experimental curve properly: the shunt current mainly describes the reverse region, while the exponential current explains the transition to the ideal exponential term in the forward region. Because the exponential factor remains unchanged throughout the temperature range studied, we can conclude that the exponential term is related to a tunneling mechanism.

In the medium forward voltage range [$0.4 < V_D(V) < 0.7$], the reverse saturation current density and the exponential factor values obtained at room temperature from the fitting ($J_{S1}=20\ pA/cm^2$, $A_1=35.2$) are very different from the values obtained when it is assumed that the total current is due to a single dominant mechanism ($J_{S1}=260\ pA/cm^2$, $A_1=29.8$). The change in the slopes given by the exponential

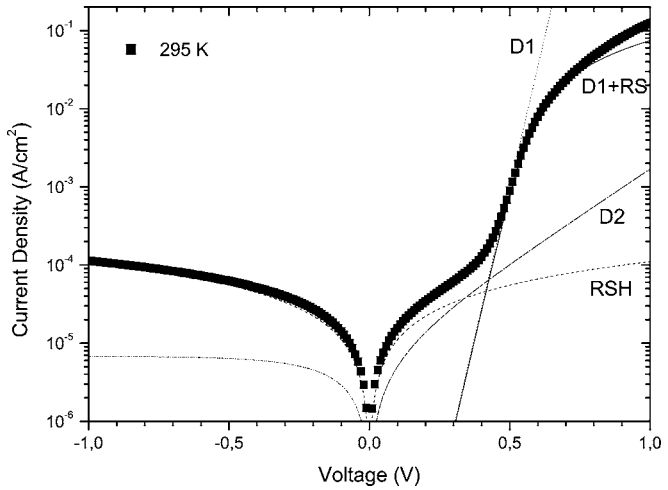

FIG. 5. Experimental (symbols) dark current-voltage characteristics at room temperature. The contribution of each conduction mechanism is shown separately.

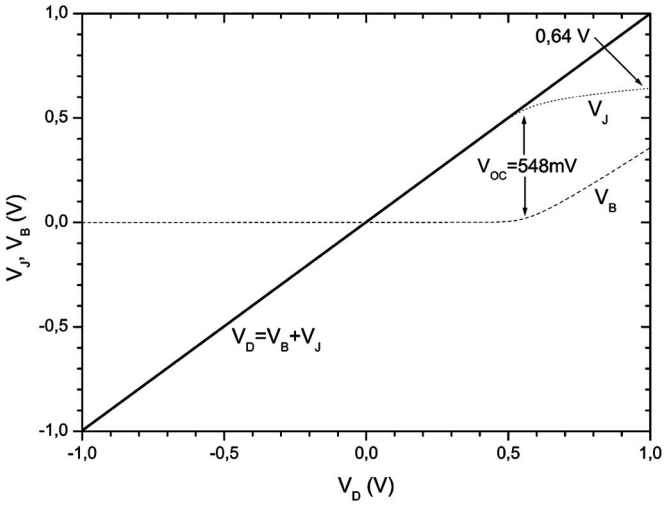

FIG. 6. Junction (V_J) and bulk (V_B) voltage variations with applied voltage (V_D). The junction voltage drop (0.64 V at V_D=1 V) and the open-circuit voltage are shown.

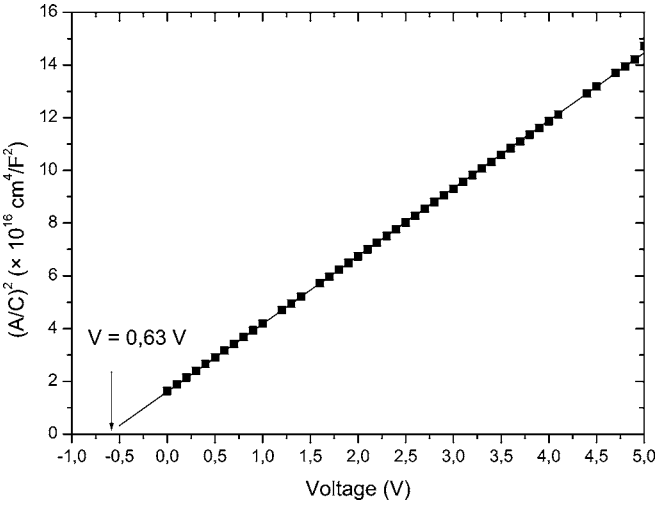

FIG. 7. Experimental (symbols) and fitted (line) capacitance-voltage characteristics at room temperature. The calculated diffusion voltage (0.63 V) is shown.

factor A forces the very different J_S values. It is also important to notice that the activation energy of the saturation current also changes from 1.08 eV (compact model) to 0.79 eV (simplified model). In both models, we can assume that the current in this voltage range is limited by diffusion in the crystalline region. However, the values obtained by using the equivalent circuit proposed in this study give an ideality factor and an activation energy that are closer to the ideal values (A=38.7 and E_{act}=1.12 eV) than those obtained when the simplified model is assumed.

The series resistance value obtained from the fitting (R_s=5.0Ω) is very close to the series resistance measured from the solar cell under AM 1.5 illumination (R_s=4.9Ω) but not to the one measured from the simplified model (R_s =3.9Ω). This might be another validation of the robustness of the equivalent circuit proposed. It should be pointed out that the series resistance effects are important at forward voltages greater than 0.4 V, in both light and dark conditions. The series resistance, but not the SCLC, limits the dark current-voltage plot in the medium forward voltage range, $0.4 < V_D(\mathrm{V}) < 0.7$. In addition, the conductivity of the a-SiC:H layer improves due to the photogenerated carriers (10^{-6} S/cm dark, 10^{-5} S/cm light).[25] These results may explain why the solar cell J-V characteristics are not affected by the SCLC but are still limited by the series resistance.

Figure 6 shows the calculated partition of the applied voltage between the junction (V_J) and the bulk (V_B) at room temperature. At reverse and low forward voltages, the voltage drop in the bulk is negligible so, in this region, the current-voltage characteristics are junction controlled. On the other hand, at high forward voltages, the voltage drop in the bulk is important and the characteristics are bulk controlled. It is important to notice that the open-circuit voltage measured from the light characteristics (V_{OC}=548 mV) coincides with the voltage value where the bulk effects start to be non-negligible.

In devices where SCLC occurs, the density of states can be estimated from the temperature dependence of the power term m.[24] So it is very important to use the actual bulk voltage drop (V_B) instead of the total applied voltage so as not to misestimate the trap distribution.

Figure 7 shows the capacitance-voltage characteristics of the diode. The linear relationship indicates that the junction is abrupt. From the saturation of V_J vs V_D, the junction diffusion voltage can be estimated from Fig. 6 to be 0.64 V at V_D=1 V, which is in good agreement with capacitance-voltage measurements (0.63 V).

IV. CONCLUSIONS

This paper has reported a compact equivalent circuit which includes two exponential mechanisms, shunt and series resistances and space-charge limited current. The model is continuous and makes it possible to accurately fit the dark current density-voltage-temperature characteristics of non-ideal junction solar cells without assuming dominating current mechanisms.

As an example of an application, a p+a-SiC:H/n c-Si solar cell has been studied in detail. In this particular case, but without losing any generality, the drop voltage in the junction and the drop voltage in the bulk can be accurately calculated by the fitting procedure, and this makes it possible to obtain physical interpretations about the origin of the open-circuit voltage of the solar cell and the diffusion potential of the junction

ACKNOWLEDGMENT

This work was supported by the Spanish Commission of Science and Technology (CICYT) under Grant No. TIC2005-02038.

[1] S. M. Sze, *Physics of Semiconductor Devices*, 2nd ed. (Wiley, New York, 1981).
[2] A. Ortiz-Conde and F. J. Garcia, Solid-State Electron. **49**, 465 (2005).
[3] J. Merten, J. M. Asensi, C. Voz, A. V. Shah, and J. Andreu, IEEE Trans. Electron Devices **45**, 423 (1998).
[4] H. Matsuura, T. Okuno, H. Okushi, and K. Tanaka, J. Appl. Phys. **55**, 1012 (1984).

[5]K. Araki and M. Yamaguchi, Sol. Energy Mater. Sol. Cells **75**, 457 (2003).
[6]J. H. Tan and W. A. Anderson, Sol. Energy Mater. Sol. Cells **77**, 283 (2003).
[7]B. Mazhari, Sol. Energy Mater. Sol. Cells **90**, 1021 (2006).
[8]A. Rose, Phys. Rev. **97**, 1538 (1955).
[9]D. Chirvase, Z. Chiguvare, M. Knipper, J. Parisi, V. Dyakonov, and J. C. Hummelen, Synth. Met. **138**, 299 (2003).
[10]M. M. El-Nahass, H. M. Zeyada, M. S. Aziz, and N. A. El-Ghamaz, Solid-State Electron. **49**, 1314 (2005).
[11]F. Schauer, Sol. Energy Mater. Sol. Cells **87**, 235 (2005).
[12]S. C. Jain, T. Aernout, A. K. Kapoor, V. Kumar, W. Geens, J. Poortmans, and R. Mertens, Synth. Met. **148**, 245 (2005).
[13]M. S. Roy, Manmeeta, P. Jaiswal, and G. D. Sharma, J. Appl. Phys. **94**, 7692 (2003).
[14]V. Kumar, S. C. Jain, A. K. Kapoor, J. Poortmans, and R. Mertens, J. Appl. Phys. **94**, 1283 (2003).
[15]J. Zhu, V. L. Dalal, M. A. Ring, J. J. Gutierrez, and J. D. Cohen, J. Non-Cryst. Solids **338–340**, 651 (2004).
[16]A. M. Eppler, I. M. Ballard, and J. Nelson, Physica E (Amsterdam) **14**, 197 (2002).
[17]L. F. Marsal, I. Martin, J. Pallarès, A. Orpella, and R. Alcubilla, J. Appl. Phys. **94**, 2622 (2003).
[18]P. Rosales-Quintero, A. Torres-Jacome, R. Murphy-Arteaga, and M. Landa-Vázquez, Semicond. Sci. Technol. **19**, 366 (2004).
[19]Z. Shen, U. Kortshagen, and S. A. Campbell, J. Appl. Phys. **96**, 2204 (2004).
[20]M. A. Rafiq, Y. Tsuchiya, H. Mizuta, S. Oda, S. Uno, Z. A. K. Durrani, and W. I. Milne, Appl. Phys. Lett. **87**, 182101 (2005).
[21]R. A. M. Hikmet, D. V. Talapin, and H. Weller, J. Appl. Phys. **93**, 3509 (2003).
[22]R. W. I. de Boer, M. Jochemsen, T. M. Klapwijk, A. F. Morpurgo, J. Niemax, A. K. Tripathi, and J. Pflaum, J. Appl. Phys. **95**, 1196 (2004).
[23]A. Goldenblum, I. Pintilie, M. Buda, A. Popa, T. Botila, A. Dimoulas, and G. Vellianitis, Appl. Phys. Lett. **86**, 203506 (2005).
[24]L. F. Marsal, J. Pallarès, X. Correig, J. Calderer, and R. Alcubilla, Semicond. Sci. Technol. **11**, 1209 (1996).
[25]J. Pallarès and R. E. I. Schropp, J. Appl. Phys. **88**, 293 (2000).